

Simone Genovesi, *Member, IEEE*, Filippo Costa, *Member, IEEE* and Agostino Monorchio, *Fellow, IEEE*

Chipless RFID Tag Exploiting Multifrequency Delta-Phase Quantization Encoding

Abstract—A novel encoding paradigm for chipless RFID tags based on phase quantization is presented. The most distinctive features of this approach are represented by the low requirement on bandwidth and by the encoding scheme. The former is achieved by using only a multi-frequency reading without resorting to ultra-wideband systems whereas the latter relies on linking the information to the quantized difference between the TE and TM phase response of the tag. The encoding mechanism is described as well as the decoding procedure. The reliability of the illustrated approach is experimentally validated by measurements on fabricated prototypes.

Index Terms—Radio Frequency Identification (RFID), chipless RFID, differential codification.

I. INTRODUCTION

Tracking of goods, people localization, remote identification, access control are only some of the multiple applications in which Radio Frequency Identification (RFID) has been exploited in the recent years [1], [2]. Commercialized RFID tags are mainly passive and consist of an antenna connected to a chip. The probing/interrogating wave coming from the antenna reader induces in the antenna tag an electrical current able to power the integrated circuit which in turns modulates the backscattered signal collected by the reader. Although the cost of the RFID tags is low, it is desirable to decrease even further for tagging low-price items. To match these needs, chipless RFID tags have been considered as an alternative to the barcode and to the tag equipped with a chip being a good trade-off in terms of low cost and operational potential[3]–[5]. Chipless RFID are simple to fabricate and do not employ damageable IC thus they are also suitable to be used in harsh environments or in extreme conditions. The information is still embedded in the electromagnetic response of the tag but, in the absence of a modulating chip, chipless RFID systems generally require an increased reader complexity in order to extract the encoded data. The definition of a unique electromagnetic footprint of each chipless RFID tag has been obtained by exploiting several different approaches. The positioning of deep nulls in the amplitude of the tag frequency response is employed in [5] and [6] for encoding the data. Time-domain techniques are proposed in [8], [9] to extract the information from the chipless response. The phase response is exploited in [10] whereas cross-polar components are used in [11],[12]. Hybrid approaches and other paradigms are illustrated in [13],[14], [15]. This paper illustrates the design of a chipless RFID tag that encodes the information by discretizing the difference (*delta-phase*) between the phase of the reflection coefficient for a TE and a TM plane wave incidence. This solution provides a tag with a reliable coding with respect to the polarization of the incident field. The footprint of the tag can also be considered small if compared to the most part of existing chipless tags. Moreover, the presence of a ground

plane in the tag guarantees a configuration less prone to detuning effects due to tagged objects.

A relevant distinctive feature is the small amount of bandwidth required since the encoding mechanism exploits only a few fixed frequencies. The reading can be therefore performed by a multi-frequency system without resorting to ultra-wideband readers.

This letter is organized as follows. Section II describes the delta-phase quantization encoding strategy and Section III provides the details for the design. Experimental results are presented in Section IV whereas conclusions are drawn in Section V.

II. DIFFERENTIAL PHASE-ENCODED CONCEPT

To introduce the delta-phase quantization encoding concept, let us consider the phase response of the periodic surface whose rectangular unit cell is shown in Fig. 1 when illuminated, at normal incidence, both with a TE plane (E-field parallel to x-axis) wave and a TM plane wave (H-field parallel to x-axis). The structure comprises a grounded dielectric substrate with a rectangular loop printed on the top face. A stub of length S is attached in correspondence of each loop corner. The periodicity of the unit cell is equal to $T_x = 1.5$ cm and $T_y = 2$ cm along x and y axis, respectively (Fig. 1). The dimension of the rectangular loop is equal to D_x in x -direction and D_y in y -direction.

The unit cell is discretized into 64×64 pixel matrix for the analysis with a Periodic Method of Moments (PMM) [16]. The width of the rectangular ring and the stub is one pixel, as well as the space between the ring side and the stub. Let us fix the dimension $D_x = 58$ pixel and $D_y = 62$ pixel and look the phase response for two different values of stub length, $S_1 = 12$ pixel and $S_2 = 16$ pixel. The periodic surface is printed on a FR4 dielectric slab ($\epsilon_r = 4.4 - j0.088$) of thickness $h = 3.6$ mm.

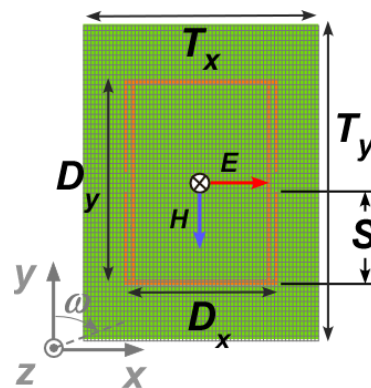


Fig. 1 – Top view of the single-loop unit cell of the periodic surface. For a TE plane wave normally impinging on the surface the electric field E is parallel to x axis. The 64×64 pixel grid employed by the PMM is shown as well. Angle ω is measured with respect to y axis.

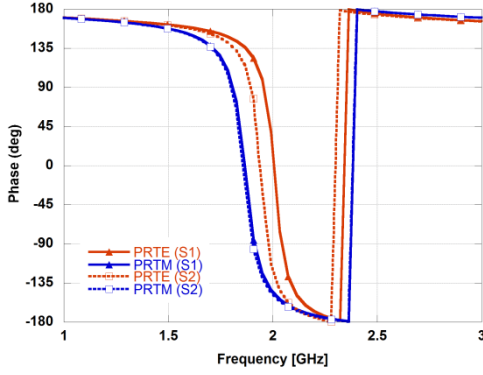


Fig. 2 – The phase of the reflection coefficient for both a TE (*PRTE*) and TM (*PRTM*) plane wave incidence impinging on the periodic surface.

Looking at the phase response in Fig. 2, it can be noticed that even a small change in the stub length leads an evident shift of the phase response for a TE incident plane wave whereas the TM response is almost unaffected. The difference between the TE and TM response is shown in Fig. 3. As highlighted in the plot, it is possible to exploit the delta-phase associated to a particular stub length as a bit codification.

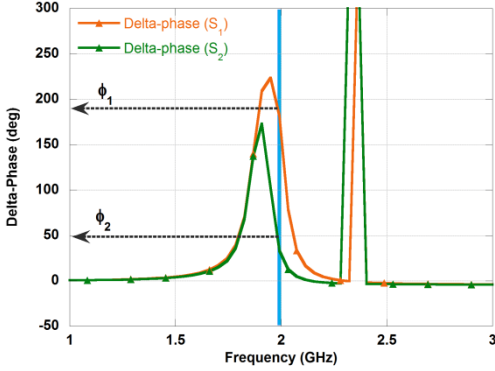


Fig. 3 – Delta-phase response for the two stub lengths, S_1 and S_2 . Frequency f_i is highlighted in blue colour.

For example, the differential phases exhibited at frequency $f_i = 2$ GHz for the two stub lengths S_1 and S_2 are ϕ_1 and ϕ_2 and more values can be obtained with different stub lengths. Let us change the stub length and look at the delta-phase value exhibited at frequency f_i . The length is expressed by using the number of pixels composing the stub (Fig. 4). It can be seen that the delta-phase value spans within the interval $(-25^\circ, 250^\circ)$, with short stubs exhibiting the highest differential phase values. Therefore a stub can encode a multi-value bit with more than two states. The set of stub lengths employed in the codification depends on the criterion used for quantizing and discriminating two phase states. The stubs whose delta-phase differs at least Δ degrees is adopted. It is apparent from Fig. 4 that 10 stub lengths will be available if $\Delta = 10^\circ$ whereas keeping $\Delta = 20^\circ$ or 30° the different selectable states will be 8 and 6, respectively. This means that one stubbed ring allows codifying 3 bits if $\Delta = 20^\circ$ is chosen.

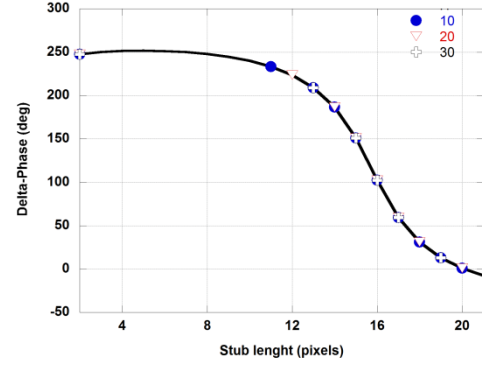


Fig. 4 – Quantization of delta-phase at the fixed frequency f_i for different stub lengths. Pixels are defined as cell periodicity D_y over 64.

The final step is to define the decoding procedure. Let us consider again the delta-phase ϕ at frequency f_i . for $\Delta = 20^\circ$. This choice individuates a set of delta-phases within the interval $[\phi - \Delta/2, \phi + \Delta/2]$, where if $\Delta/2$ is the accepted phase deviation. The individuated intervals do not intersect thus there is no ambiguity in the reading process.

Finally, it is interesting to define the effect of the incident wave angle on the delta-phase behavior. The proposed codification can be employed up to $\omega = 25^\circ$ and $\theta = \pm 30^\circ$.

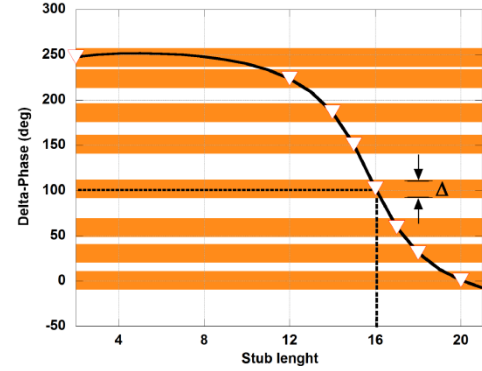


Fig. 5 – Decision intervals of the quantized delta-phase defined by a fixed Δ . In this case a stub length =16 produces a differential phase of 100° . The information is considered correctly retrieved if the measures delta-phase response is within $[100^\circ - \Delta/2, 100^\circ + \Delta/2]$.

III. CHIPLESS TAG DESIGN

In order to increase the quantity of information stored in the chipless tag, a structure with four nested rings has been investigated (Fig. 6). Each ring J , has its own stubs S^J of equal length attached to the corner and obviously different $D_{x,J}$ and $D_{y,J}$. In this case the codification of the information is related to the differential phase exhibited by the tag at four fixed frequencies f_i ($i = 1,2,3,4$).

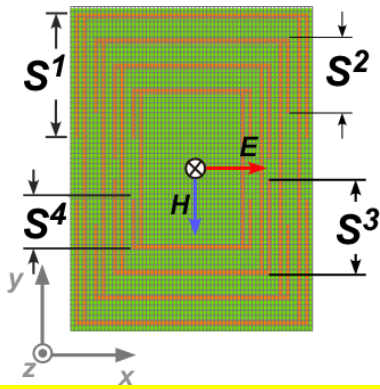


Fig. 6 – Top view of the multi-loop unit cell of the proposed periodic surface.

In order to evaluate the robustness of the employed unit cell configuration it is important to verify that the differential phase response of one ring is not altered by the change in the stub lengths of the other elements. Let us consider, for example, a critical case when the first three stubs fixed with intermediate lengths ($S^1 = 12$, $S^2 = 8$ and $S^3 = 7$) and the fourth spanning from 3 to 15 pixel. It can be seen that the delta-phase curve is changing only in correspondence of the peak #4, the one associated to the fourth ring.

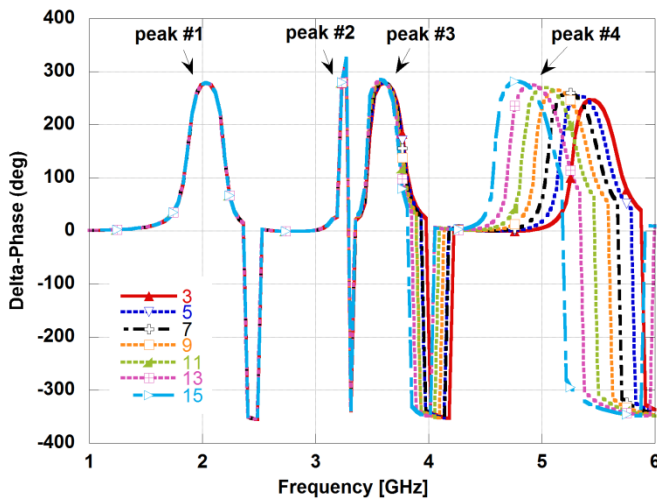


Fig. 7 – Variation of the delta-phase response for a structure with the first three stubs fixed ($S^1 = 12$, $S^2 = 8$ and $S^3 = 7$) and the fourth spanning from 3 to 15 pixel.

Therefore the change in the delta-phase exhibited at the frequencies f_i is mostly related to the stub length of the corresponding ring and it is weakly related to the adjacent elements. The behavior is confirmed when the current distribution on the unit cell at the four design frequencies is observed (Fig. 8). The frequencies f_i and the relevant pixel-lengths for describing the structure are summarized in Table I.

TABLE I
PIXEL DIMENSION OF EACH RING AND CONNECTED STUB

Element#1	Element#2	Element#3	Element#4
$D_{x1} = 58$	$D_{x2} = 48$	$D_{x3} = 38$	$D_{x4} = 28$
$D_{y1} = 62$	$D_{y2} = 52$	$D_{y3} = 42$	$D_{y4} = 32$
$S^1 = 12$	$S^2 = 8$	$S^3 = 7$	$S^4 = 13$
$f_1 = 2$ GHz	$f_2 = 2.86$ GHz	$f_3 = 3.82$ GHz	$f_4 = 4.93$ GHz

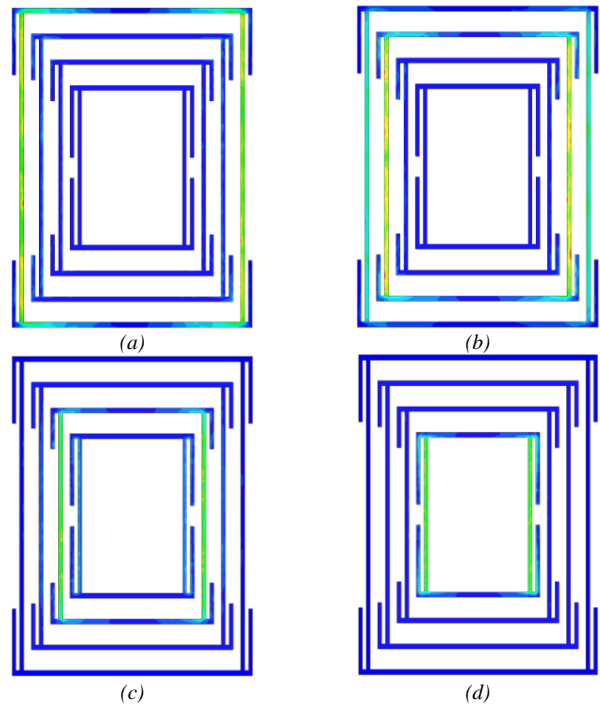


Fig. 8 – Normalized current distribution at the resonance of (a) element#1 at f_1 , (b) element#2 at f_2 , (c) element#3 at f_3 and (d) element#4 at f_4 .

Let us now calculate the number of states encoded by the described structure. Considering $\Delta = 10^\circ$ the total number of combinations is equal to 13104, that is 13.67 bits, whereas by choosing $\Delta = 30^\circ$ the bit number is 10.49. Contrarily to many encoding schemes that require an ultra-wide or wide band occupation, the proposed codification paradigm requires the chipless RFID tag phase response at 4 fixed frequencies only. Therefore, the number of bits/MHz allocated at a single frequency spans from 3.41 to 2.62, for $\Delta = 10^\circ$ and $\Delta = 30^\circ$, respectively (Table II).

TABLE II
QUANTIZED DELTA-PHASE VALUES OBTAINED FOR DIFFERENT Δ FOR A CHIPLESS RFID REALIZED ON THE FR4 SUBSTRATE

	$\Delta = 10^\circ$	$\Delta = 20^\circ$	$\Delta = 30^\circ$
Element#1	13	10	8
Element#2	9	5	4
Element#3	14	12	9
Element#4	8	6	5
combinations	13104	3600	1440
bits	13.67	11.81	10.49
bits/Band.	3.41	2.95	2.62

Finally, it is remarked that a substrate with a lower dielectric permittivity, such as Teflon ($\epsilon_r = 2.17 - j0.0022$) could guarantee a less steep phase response and therefore more discrete-phase states are available. By considering the same unit cell size (T_x, T_y), more combinations are obtained (Table III) although the f_i frequencies are obviously shifted at higher values ($f_1 = 2.8$ GHz, $f_2 = 4$ GHz, $f_3 = 5.1$ GHz, $f_4 = 6.5$ GHz). In particular, the number of combinations is almost doubled for $\Delta = 10$ and almost tripled for $\Delta = 30$.

TABLE III

QUANTIZED DELTA-PHASE VALUES OBTAINED FOR DIFFERENT Δ FOR A CHIPLESS RFID REALIZED ON THE TEFLON SUBSTRATE

	$\Delta=10^\circ$	$\Delta=20^\circ$	$\Delta=30^\circ$
Element#1	18	11	9
Element#2	15	12	11
Element#3	12	11	8
Element#4	8	6	5
combinations	25920	8712	3960
bits	14.66	13	11.95
bits/Band.	3.67	3.25	2.99

IV. EXPERIMENTAL RESULTS

Several chipless RFID tags have been fabricated and measured to assess the performance of the proposed quantized delta-phase encoding scheme. A finite-size tag comprising 3x3 unit cells has been reported in Fig. 9a as a representative example. The tag has been placed at 50 cm in front of two dual-polarized wideband horn antennas (Flann DP280). An Agilent E5071C vector network analyzer has been employed for collecting the scattering parameters in a non-anechoic environment [6]. Fig. 9b reports a measured frequency response with the occupied frequency band highlighted with blue vertical bars. It is important to highlight that only these frequencies are employed in the reading process since the delta-phase encoding needs only a few fixed frequencies. Therefore, the reader is based on a multi-frequency narrow-band probe avoiding wideband or ultra-wideband radiators.

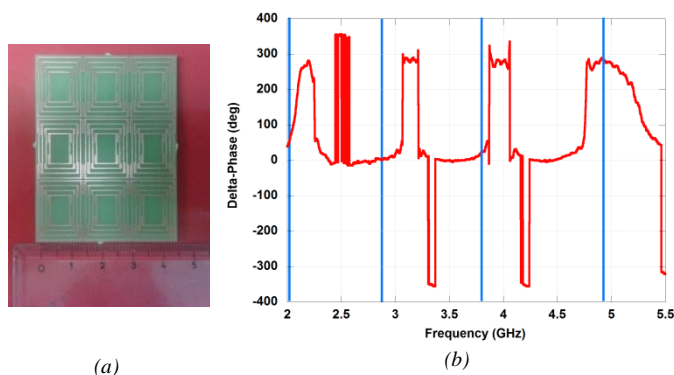


Fig. 9 – Prototype of the chipless RFID tag comprising 3x3 unit cells (a) and quantized phase encoding (b) (frequencies f_i are highlighted in blue).

TABLE IV

COMPARISON BETWEEN SIMULATIONS AND MEASUREMENTS

Element#	Stub length (pixel)	Simulated delta phase (deg)	Measured delta phase (deg)	Error (deg)
1	15	22	30	8
2	12	6	3.5	2.5
3	10	7	16	9
4	13	275	284	9

Indeed, the more cells are employed the higher is the physical footprint of the tag and thus the radar cross section. By using a 3x3 unit cells tag we have obtained a read range of 50 cm with an input power of 0 dBm. A longer read-range can be achieved by using more unit cells (*i.e.* 4x4 or 5x5) for each

tag [6]. The comparison between simulation and measurements for the chipless RFID tag comprising 3x3 unit cells is provided in Table IV. Similar performance have been observed in all the manufactured tags and suggest that a $\Delta = 20^\circ$ can be considered a good choice able to guarantee the trade-off between encoding capacity and correct recovering of the information.

V. CONCLUSION

A new chipless RFID tag based on a quantized delta-phase encoding has been illustrated. The information is encoded in the quantized values of the difference between the TE and TM phase response. This encoding paradigm has low requirement on bandwidth and it can be implemented by a multi-frequency reader without resorting to ultra-wideband systems. The performance have been assessed by measurements on fabricated prototypes.

REFERENCES

- [1] K. Finkenzeller, *RFID Handbook: Radio-frequency Identification Fundamentals and Applications*. Wiley, 2004.
- [2] C. Occhiuzzi, S. Caizzone, and G. Marocco, "Passive UHF RFID antennas for sensing applications: Principles, methods, and classifications," *Antennas Propag. Mag. IEEE*, vol. 55, no. 6, pp. 14–34, 2013.
- [3] R. R. Fletcher, "Low-cost electromagnetic tagging: design and implementation," Thesis, Massachusetts Institute of Technology, 2002.
- [4] S. Tedjini, N. Karmakar, E. Perret, A. Vena, R. Koswatta, and R. E-Azim, "Hold the Chips: Chipless Technology, an Alternative Technique for RFID," *IEEE Microw. Mag.*, vol. 14, no. 5, pp. 56–65, Jul. 2013.
- [5] S. Preradovic and N. C. Karmakar, "Chipless RFID: Bar Code of the Future," *Microw. Mag. IEEE*, vol. 11, no. 7, pp. 87–97, 2010.
- [6] F. Costa, S. Genovesi, and A. Monorchio, "A Chipless RFID Based on Multiresonant High-Impedance Surfaces," *IEEE Trans. Microw. Theory Tech.*, vol. PP, no. 99, pp. 1–8, 2012.
- [7] S. Preradovic, I. Balbin, N. C. Karmakar, and G. F. Swiegers, "Multiresonator-Based Chipless RFID System for Low-Cost Item Tracking," *IEEE Trans. Microw. Theory Tech.*, vol. 57, no. 5, pp. 1411–1419, May 2009.
- [8] A. T. Blischak and M. Manteghi, "Embedded Singularity Chipless RFID Tags," *IEEE Trans. Antennas Propag.*, vol. 59, no. 11, pp. 3961–3968, Nov. 2011.
- [9] A. Ramos, A. Lazaro, D. Girbau, and R. Villarino, "Time-Domain Measurement of Time-Coded UWB Chipless RFID Tags," *Prog. Electromagn. Res.*, vol. 116, 2011.
- [10] I. Balbin and N. C. Karmakar, "Phase-Encoded Chipless RFID Transponder for Large-Scale Low-Cost Applications," *IEEE Microw. Wirel. Compon. Lett.*, vol. 19, no. 8, pp. 509–511, Aug. 2009.
- [11] F. Costa, S. Genovesi, and A. Monorchio, "Chipless RFIDs for Metallic Objects by using Cross Polarization Encoding," *IEEE Trans. Antennas Propag.*, vol. Early Access Online, 2014.
- [12] A. Vena, E. Perret, and S. Tedjini, "A Depolarizing Chipless RFID Tag for Robust Detection and Its FCC Compliant UWB Reading System," *IEEE Trans. Microw. Theory Tech.*, vol. 61, no. 8, pp. 2982–2994, Aug. 2013.
- [13] A. Vena, E. Perret, and S. Tedjini, "Chipless RFID Tag Using Hybrid Coding Technique," *IEEE Trans. Microw. Theory Tech.*, vol. 59, no. 12, pp. 3356–3364, Dec. 2011.
- [14] A. Lazaro, A. Ramos, D. Girbau, and R. Villarino, "Chipless UWB RFID Tag Detection Using Continuous Wavelet Transform," *IEEE Antennas Wirel. Propag. Lett.*, vol. 10, pp. 520–523, 2011.
- [15] C. Mandel, B. Kubina, M. Schüßler, and R. Jakoby, "Metamaterial-inspired passive chipless radio-frequency identification and wireless sensing," *Ann. Telecommun. - Ann. Télécommunications*, vol. 68, no. 7–8, pp. 385–399, Aug. 2013.
- [16] R. Mittra, C. H. Chan, and T. Cwik, "Techniques for analyzing frequency selective surfaces—a review," *Proc. IEEE*, vol. 76, no. 12, pp. 1593–1615, Dec. 1988.